Forging Ru-C_{sp2} Bonds in Paddlewheel Complexes Using the Lithium-

Halogen Exchange Reaction

Adharsh Raghavan, Brandon L. Mash and Tong Ren *

Department of Chemistry, Purdue University, West Lafayette, Indiana 47907, United States

Abstract: Reported herein are the first examples of the formation of Ru–C_{sp2} bond in paddlewheel diruthenium species. A series of six Ru₂(ap)₄(C₆H₄-4-X) type compounds (ap = 2-aniliopyridinate; $X = NMe_2$ (1); N,N-(C₆H₄-4-OMe)₂ (2); ^tBu (3); H (4); Br (5); CF₃ (6)) was synthesized by employing the lithium-halogen exchange reaction with a variety of parasubstituted haloaryl ligands. These compounds have been characterized via electronic absorption spectroscopy, cyclic voltammetry, mass spectrometry, magnetism studies, and their molecular structures established by single crystal X-ray diffraction studies. All compounds are in the Ru₂⁵⁺ oxidation state, with a ground state electronic configuration of $\sigma^2 \pi^4 \delta^2 (\pi^* \delta^*)^3$. Crystal structures of 1–6 confirm this, indicating a Ru–Ru bond order of 2.5. Electrochemical data suggests that the σ-aryls are stronger donors than σ-alkynyls. A range of electronically different substituents allows for a closer inspection of the extent of electronic conjugation across the diruthenium

 * To whom correspondence should be addressed. E-mail: $\underline{\text{tren@purdue.edu}}$

paddlewheel core and the axial aryl ligand.

.

Introduction

Diruthenium paddlewheel complexes have been extensively studied since the isolation of Ru₂(acetate)₄Cl in 1966 by Wilkinson.^{1,2} The earliest example of their organometallic congener came from the Cotton group in 1986, namely, $Ru_2(ap)_4(C \equiv CPh)$ (where ap = 2anilinopyridinate).³ Since then, interest has burgeoned in the study of Ru₂L₄(C≡CR)_n type complexes (n=1 or 2). Because of the extended conjugation along the Ru₂-poly-alkynyl chains and the robust redox states of the Ru_2^{n+} (n = 4, 5 or 6) paddlewheel motif, the wire-like characteristics of these molecules, many of which are based on Ru₂(ap)₄, have been studied by several laboratories including ours. 5-11 This has enabled incorporation of Ru₂(ap)₄-alkynyl molecules in non-volatile flash memory devices. 12,13 The diverse utility of Ru₂(ap)₄ containing molecules in forming Ru-Ru-Oxo species and capturing the exotic anion AgF₂ has been demonstrated by Berry and co-workers. 14-16 It is noteworthy that all structurally characterized organometallic diruthenium paddlewheel complexes feature either one or two alkynyl axial ligand(s),⁴ or smaller ligands like CN⁻¹⁷ or CO.¹⁸ Specifically, the Ru-Ru-C_{sp2} bond in a paddlewheel motif is a much sought-after target, since nothing is known about the bonding, structure and reactivity of these species.

The existence of Rh–Rh–C_{sp²} bonds in paddlewheel compounds has indeed been documented by the laboratories of Doyle and Bear-Kadish. Doyle and co-workers first reported the synthesis and characterization of a bis(phenyl)dirhodium(III) compound formed *via* oxidation of a Rh₂(II,III) species in the presence of NaBPh₄. The compound is diamagnetic, as is expected from Rh₂⁶⁺. However, the disappearance of the Rh–Rh bond is unexpected, which denotes a change in the electronic structure of the Rh₂ core. Since then, other reagents like

arylboronic acids have been employed to introduce a wider range of substituents in the axial sites of Rh₂(III,III) caprolactamates. ²⁰⁻²² The electronic configuration of Rh₂⁶⁺ in these compounds has been established as $\pi^4 \delta^2 \pi^{*4} \delta^{*2}$. ²² In 2009, Bear and Kadish reported the synthesis of mono-aryl and mono-alkyl compounds Rh₂(ap)₄(C₆H₅) and Rh₂(ap)₄(CH₃) from Rh₂(ap)₄Cl using large excesses of phenyllithium and methyllithium, respectively. ²³ However, product isolation required a rigorously inert atmosphere and sequestration from any light source to avoid decomposition of the relatively unstable compounds. It is worth noting that rich chemistry related to the formation of Ru–C_{sp2} bond in Ru₃ clusters, though not of paddlewheel motif, has been described by Cabeza and coworkers. ^{24,25}

Despite the similarity between dirhodium and diruthenium paddlewheel complexes, it is noteworthy that there is no precedent in literature for diruthenium compounds bearing axial σ -aryl ligands. The only example of a diruthenium aryl compound comes from the Cotton group. The compound with the formula Ru₂Ph₂(PhCONH)₂[Ph₂POC(Ph)N]₂ was prepared from the reaction between Ru₂(PhCONH)₄Cl and PPh₃, and the transfer of a Ph group from the axially coordinated PPh₃ to Ru was accompanied by a structural rearrangement from a paddlewheel motif to an edge-sharing bioctahedral motif. It was of interest to us to synthesize diruthenium compounds containing aryl ligands in the axial positions, while leaving the paddlewheel motif unchanged. The classic technique used to forge Ru–C=C bonds involves using LiC=CR formed *via* lithiation of the corresponding alkyne, HC=CR. Hence, the well-documented lithium-halogen exchange reaction is described herein for the introduction of an aryl ligand (Ar), which has resulted in a series of Ru₂(ap)₄(Ar) in relatively high yield (Scheme 1 below).

Results and Discussion

Synthesis. Reaction between $Ru_2(ap)_4Cl$ and LiAr resulted in the formation of $Ru_2(ap)_4(Ar)$ and LiCl (Scheme 1). The reactions were instantaneous and were accompanied by easily identifiable color changes. Work-up of the reaction mixtures and purification of the products were done under ambient conditions, using column chromatography or by simple recrystallization techniques; products were isolated in yields ranging from 30-95%. Since $[Ru_2(ap)_4]$ -based compounds either decompose when exposed to the acidic surface of silica or become irretrievably adsorbed onto it, the silica used for thin-layer chromatography and column chromatography were deactivated with triethylamine prior to use. The synthesis of the analogous compound bearing 4-nitrophenyl axial ligand was attempted, but did not yield the desired product (see the supporting information). The isolated compounds 1–6 are stable both in solution (THF) and solid state under ambient conditions, with no noticeable decomposition over a few months. The effective magnetic moments of compounds 1–6 (determined using Evans method) range from 3.4 to 4.1 Bohr magneton, which are in agreement with a S = 3/2 ground state. Although their paramagnetism precluded characterization by NMR spectroscopy, compounds 1– 6 were analyzed using mass spectrometry (ESI-MS), electronic absorption spectroscopy, cyclic and differential pulse voltammetry, room temperature magnetism studies, density functional theory (DFT) calculations and single crystal X-ray diffraction studies.

Scheme 1. Synthesis of $Ru_2(ap)_4(C_6H_4-4-R)$. NN' = 2-anlinopyridinate; $R = NMe_2$ (1); $N,N-(C_6H_4-4-OMe)_2$ (2); tBu (3); H (4); Br (5); CF_3 (6)

Molecular structures. The molecular structures of compounds 1–6 determined *via* single crystal X-ray diffraction studies are shown in Figures 1–6; selected bond lengths and angles are presented in Table 1. The bridging *ap* ligands retain the (4,0) arrangement seen in $Ru_2(ap)_4C1^{.28}$ The most unique feature of the reported complexes is obviously the Ru–C bond. Compounds 1–6 feature the very first examples of Ru_2 – C_{sp^2} bonds among paddlewheel complexes. Whereas Ru_2 –C bond lengths in mono- and bis-alkynyl complexes average between 1.85–2.1 Å, compounds 1–6 all have bond lengths greater than 2.13 Å. A similar lengthening of the M–C bond is observed in the dirhodium paddlewheels $Rh_2(ap)_4(C\equiv CH)$ (Rh–C=2.021 Å) and $Rh_2(ap)_4(Ph)$ (Rh–C=2.108 Å). This increase in bond length is attributed to (i) the change in hybridization of the *ipso* carbon from sp ($r_{covalent}=69$ pm) to sp^2 ($r_{covalent}=73$ pm)²⁹ and (ii) the significant increase in sterics at the axial site from the linear $C\equiv C$ to the two-dimensional aryl. Although there is a trend of decreasing electron-donating ability of the *para* substituent upon going from compound 1 to compound 6, there is no apparent manifestation of this in the Ru–C, or the Ru–Ru bond lengths.

Ru–Ru bond lengths for the compounds range from 2.3370(5) Å to 2.3423(5) Å, and are significantly elongated from Ru₂(ap)₄Cl (2.275(6) Å).²⁸ But this is not unusual in Ru₂⁵⁺ compounds; σ -alkynyl complexes Ru₂(ap)₄((C=C)_nR) (n = 1,2) have Ru–Ru bond lengths of ca. 2.32-2.33 Å.⁴ This is attributed to the stronger electron-donor effect of the axial alkynyl ligand compared to chloro. Furthermore, the fact that it increases from 2.319(2) Å in Ru₂(ap)₄(C=CPh),³ to 2.3380(5) Å in Ru₂(ap)₄(Ph) (4) is indicative of the even stronger electron-donating ability of the aryl ligand in comparison to alkynyl. Such an effect is also seen in the case of Rh₂(ap)₄(C=CH) (Rh–Rh = 2.439 Å) vs. Rh₂(ap)₄(Ph) (Rh–Rh = 2.470 Å).²³

Not unlike alkynyls, the aryl ligands retain conjugation between the diruthenium core and the axial ligand, and this is supported by the consistent linearity of the Ru–Ru–C angles and planarity of the aryl ligands (Table 1). Except in the case of compounds 3 and 6, the aryl ligands are approximately coplanar with the plane containing Nx–Ru2–Ny (Chart 1). The two-dimensional nature of the aryl ligand is in stark contrast to the one-dimensional nature of the alkynyl ligand. This unique feature reduces the 4-fold axial symmetry observed in mono- and bis-alkynyl paddlewheel species to 2-fold, the effect of which can be seen in the electronic absorption spectra (see below).

Chart 1. Dihedral angle (θ) , defined as the angle between the lines C1–C2 and Ru2–Nx.

Table 1. Selected Bond Lengths (Å) and Angles (deg) for compounds 1–6.

	1 ^a	2	3	4 ^b	5	6^b
Ru1–Ru2	2.3347(7)	2.338(1)	2.3423(5)	2.3380(5)	2.3375(4)	2.3373(5)
Ru1–C1	2.214(3)	2.260(8)	2.190(4)	2.16(1)	2.216(5)	2.22(1)
Ru2-Ru1-C1	179.3(1)	177.8(2)	175.51(9)	173.9(3)	176.3(4)	177.9(3)
Ru1-N1	2.105(6)	2.103(8)	2.112(3)	2.104(4)	2.124(2)	2.132(4)
Ru1–N3	2.102(5)	2.118(9)	2.135(3)	2.117(4)	(Ru1-N2) 2.107(2)	2.158(9)
Ru1–N5	2.106(5)	2.118(8)	2.138(3)	2.122(4)		2.128(4)
Ru1–N7	2.109(5)	2.103(9)	2.098(3)	2.128(4)		2.106(3)
Ru2–N2	2.041(5)	2.050(7)	2.043(3)	2.062(4)	(Ru2-N3)	2.043(3)

					2.0320(19)	
Ru2-N4	2.046(5)	2.019(9)	2.041(2)	2.055(4)	2.0485(18)	2.040(4)
Ru2-N6	2.037(5)	2.045(7)	2.033(3)	2.024(4)		2.032(2)
Ru2–N8	2.051(5)	2.034(9)	2.036(2)	2.018(4)		2.038(3)
θ^c	-1.60	+4.26	-11.7	-3.79	+3.77	+10.6

^a One of the two molecules present in the asymmetric unit was chosen (Molecule A). Molecule B is shown in Figure S7; ^b major moiety chosen from disordered axial ligands. ^c θ is defined per Chart 1.

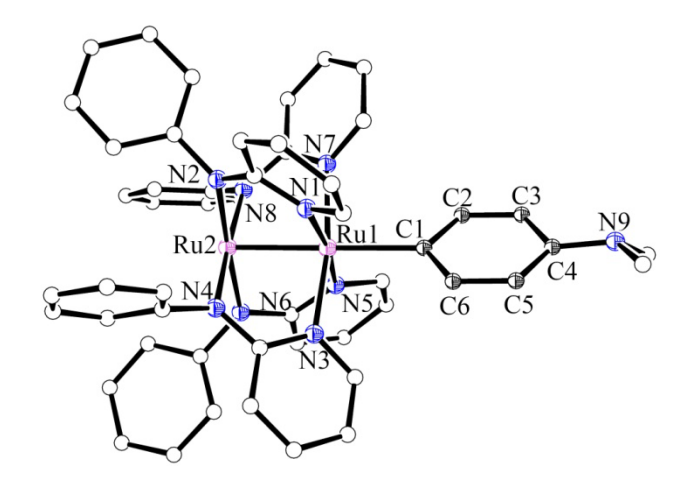


Figure 1. Structural plot of **1** at 30% probability level. One of the two molecules (A) present in the asymmetric unit was selected. Hydrogens omitted for clarity.

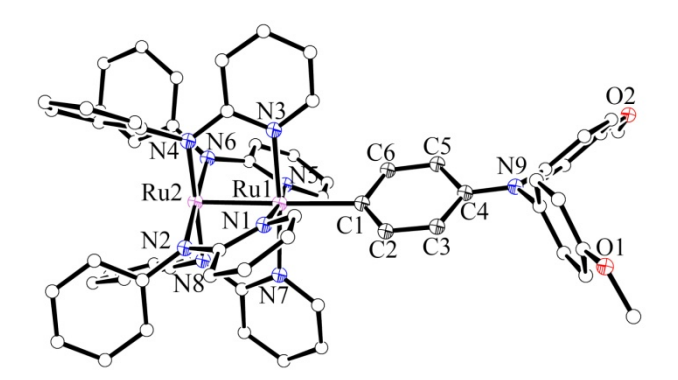


Figure 2. Structural plot of **2** at 30% probability level. Solvent molecules and hydrogens omitted for clarity.

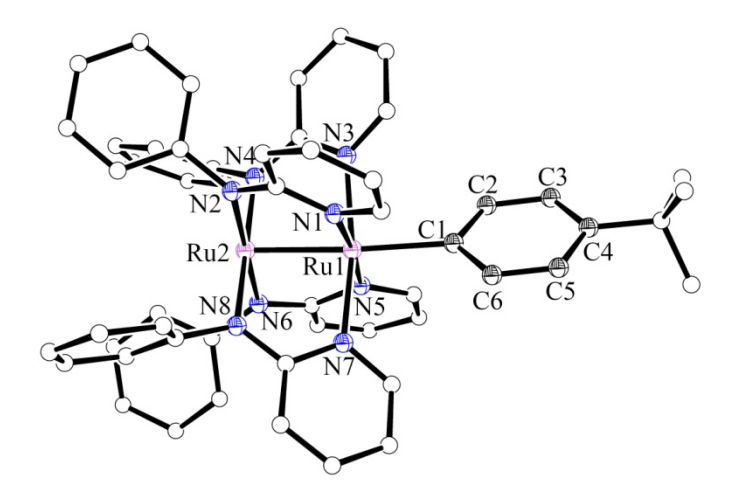


Figure 3. Structural plot of **3** at 30% probability level. Solvent molecules and hydrogens omitted for clarity.

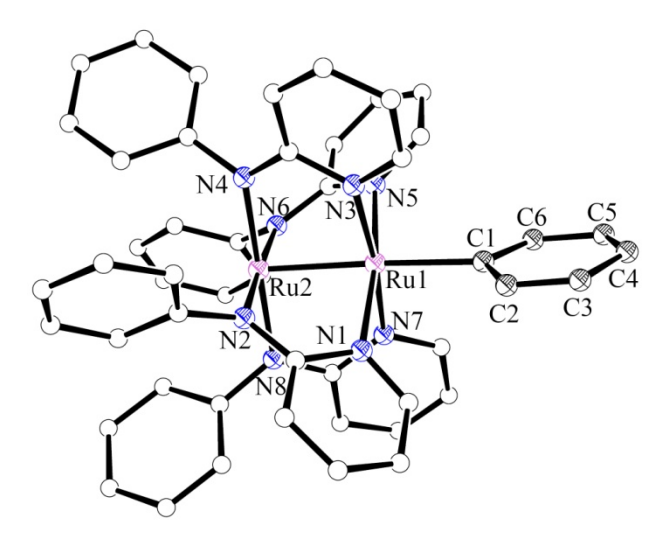


Figure 4. Structural plot of **4** at 30% probability level. Solvent molecules, disordered ligand and hydrogens omitted for clarity.

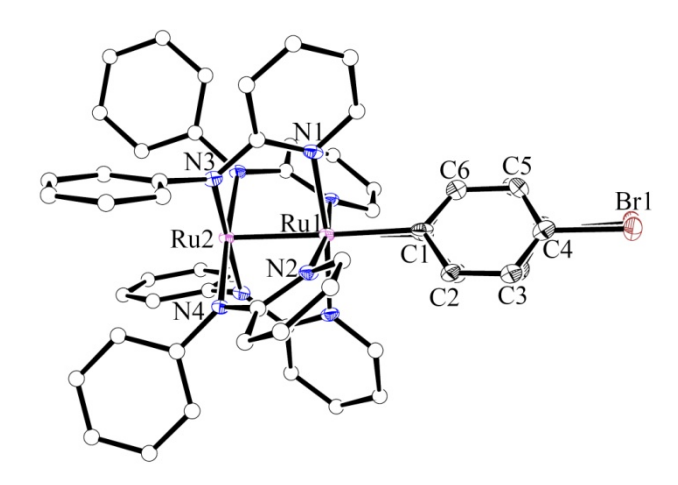


Figure 5. Structural plot of **5** at 30% probability level. Aryl ligand is disordered around the C₂ axis.

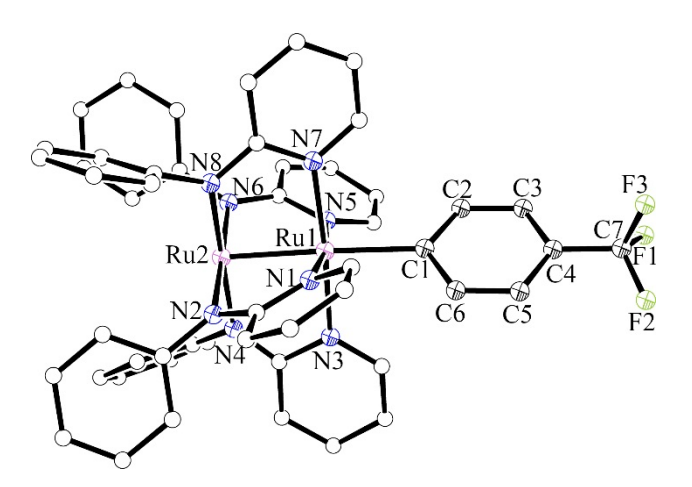


Figure 6. Structural plot of **6** at 30% probability level. Solvent molecules, disordered ligands and hydrogens omitted for clarity.

Electronic absorption spectra. All the reported compounds are intensely colored, a characteristic feature of diruthenium paddlewheels. The major features in the electronic absorption spectra of compounds 1-6 agree with those of reported Ru_2^{5+} alkynyl compounds. Figure 7 shows an overlay of the Vis-NIR absorption spectra of compounds 1-6, and $Ru_2(ap)_4Cl$.

Compounds 1–6 all undergo at least two major electronic transitions that are characteristic of Ru₂⁵⁺, one at ca. 460 nm and the other around 820 nm. Overall, the relative energies of the major absorptions are not very different from the ones seen in the starting material, Ru₂ $(ap)_4$ Cl (415 nm, 754 nm),²⁸ or in mono σ -alkynyl complexes for example, Ru₂ $(ap)_4$ (C=CPh) (415 nm, 764 nm)³ and Ru₂ $(ap)_4$ (C=CH) (466 nm, 749 nm).³⁰ The spectra of compounds 1–6 also display some subtle but unique features attributed to the axial aryl ligands.

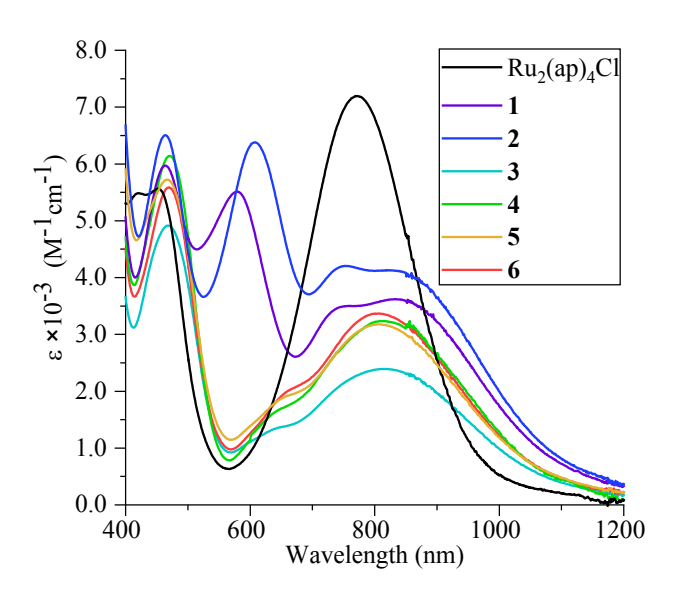


Figure 7. Vis-NIR absorption spectra of compounds 1–6 and $Ru_2(ap)_4Cl$ recorded in THF.

It is well established that the ground state configuration of $Ru_2(ap)_4L_{ax}$ is $\sigma^2\delta^2\pi^4\pi^{*2}\delta^{*1}$, and the open shell nature of this type molecules makes the assignment of transitions challenging. A recent study by Berry and coworkers based on both magnetic circular dichroism (MCD) spectroscopy and DFT calculations suggested that the peaks at 770 and 430 nm for $Ru_2(ap)_4Cl$ should be assigned as $\delta \to \pi^*$ and $\delta \to \delta^*$ transitions, respectively. It is believed that the same assignment holds true for $Ru_2(ap)_4Ar$ compounds reported here, namely, the peak at ca. 460 nm being $\delta \to \delta^*$, and the broad peak around 820 nm being $\delta \to \pi^*$. Furthermore, the latter

assignment is also consistent with the broad and even double humped (compounds 1 and 2) feature. The attachment of aryl reduces the 4-fold axial symmetry of the $Ru_2(ap)_4$ core to 2-fold, which removes the degeneracy of $\pi^*(Ru_2)$, resulting in two energetically distinctive $\delta \to \pi^*$ transitions. Conversely, the 4-fold axial symmetry is preserved in the $Ru_2(ap)_4(C_2R)$ type compounds, where a single low energy absorption has been consistently observed.

Compounds 1 and 2 display an additional intense absorption at 579 nm and 607 nm, respectively, which is the primary source of the vastly different colors of 1 (gray) and 2 (bluegreen) in comparison to those of compounds 3–6 (olive-green). This particular transition has its origin in the amino-substituent of the arvl ligand, considering that it is absent in those arvl ligands lacking an electron-donor. This is supported by the DFT calculation of 1 (see discussion below), which reveals a high-energy $\pi(Ar)$ orbital that is extensively mixed with $\pi(Ru_2)$ in SOMO-3. Therefore. the assignment for this transition is the dipole-allowed $\pi(Ru_2/Ar) \rightarrow \pi*(Ru_2/Ar)$. On the contrary, for compound 6, SOMO-3 is completely localized on the $[Ru_2(ap)_4]$ core, because the corresponding $\pi(Ar)$ orbital is likely buried at a much lower energy.

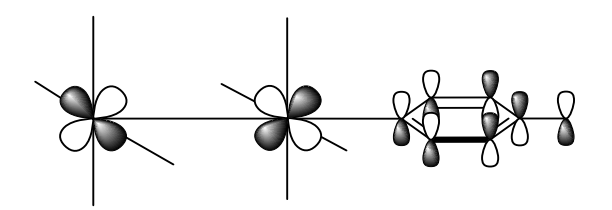


Chart 2. Representation of SOMO-3 in 1 and 2, $\pi(Ru_2)/\pi*(Ar)$.

Electrochemical studies. The redox properties of compounds **1–6** were analyzed using cyclic (CV) and differential pulse voltammetry (DPV); results are plotted in Figure 8 and

tabulated in Table 2. All compounds exhibit a reversible one-electron oxidation (**B**), corresponding to $Ru_2^{+6/+5}$, between -0.24 and -0.38 V (potentials are reported against $Fc^{+1/0}$) and a reversible one-electron reduction (**A**) corresponding to $Ru_2^{+5/+4}$, between -1.47 and -1.62 V. Compounds **1** and **2** exhibit three additional reversible one-electron oxidation events (**C**, **D** and **E**), and the oxidation at ca. 0.13 V (**C**) is attributed to the amine functionality. Two reversible one-electron oxidations at more positive potentials (**D** and **E**) occur within 0.14 V of each other, and are likely Ru_2 -centered in analogy to those described for $Ru_2(ap)_4(C_2R)$. For compounds **3**–**6**, both the one-electron reduction **A** and the first one-electron oxidation **B** are reversible. However, oxidation events beyond couple **B** (**D** and **E**) are either quasi-reversible or irreversible. While the cause of the diverse behavior of compounds **3**–**6** at more positive potentials is not straightforward, it is noteworthy that **1** and **2** are electrochemically robust even at higher potentials. The redox robustness of compounds **1** and **2** may be attributed to the ability of -NR₂ groups in stabilizing $Ru_2(ap)_4$ core at higher oxidation states through the extensive conjugation.

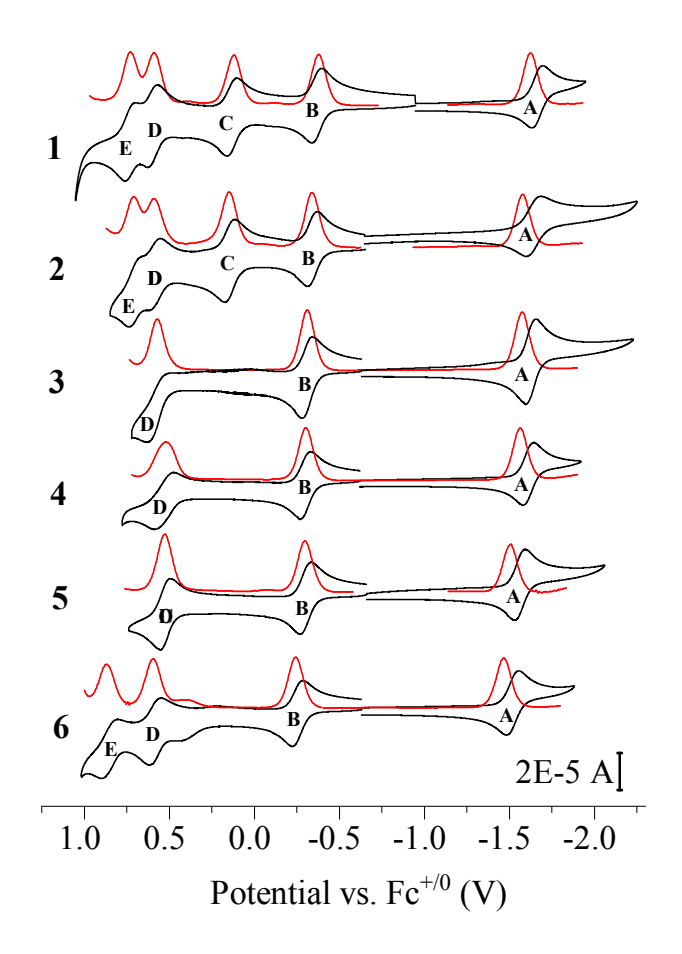


Figure 8. Cyclic (black) and differential pulse (red) voltammograms of compounds 1-6 (1.0 mM) recorded in a 0.10 M CH₂Cl₂ solution of Bu₄NPF₆ at a scan rate of 0.10 V/s.

Table 2. Electrochemical data from DPV (in V vs. Fc^{+1/0})

	A	В	C	D	E
1	-1.62	-0.38	0.12	0.59	0.73
2	-1.58	-0.34	0.15	0.59	0.71
3	-1.57	-0.31	-	0.57	-
4	-1.56	-0.30	-	0.52	-
5	-1.50	-0.29	-	0.53	-

6	-1.47	-0.24	-	0.59	0.87

It is clear from Table 2 that the potentials for reversible couples **A** and **B** shift anodically in the order **1–6**, following the trend of decreasing electron donating / increasing electron withdrawing character of the *para* substituent. The trend is further quantified through a linear fit of the first oxidation potential (E(**B**)) versus the Hammett constant of the substituents (Figure 9), ³¹⁻³³ which yields a reactivity constant (ρ) of *ca.* 98 mV (Equation 1). Similar results were obtained from Hammett plots of E(**A**) ($\rho \approx 107$ mV). Previously, the reactivity constants for the series Ru₂(*DMBA*)₄(C=C-C₆H₄-4-X)₂ (*DMBA* is *N,N'*-dimethylbenzamidinate)³⁴ were determined to be 121 mV and 86 mV for the first oxidation and reduction couples, respectively. The values of ρ are comparable between the two series, reflecting a similar impact of the *para* aryl substituents.

$$E_{1/2}(X) = \rho \sigma_x + E_{1/2}(H)$$
 (1)

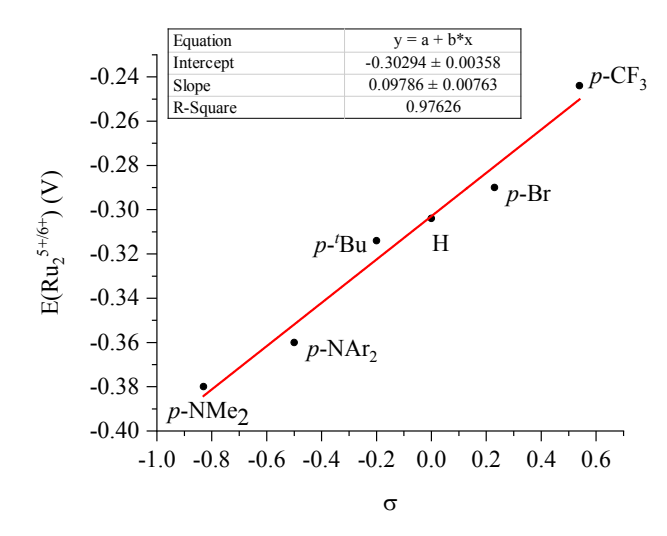


Figure 9. Hammett plot of electrode potentials ($E(Ru_2^{+6/+5})$) versus σ_x for compounds 1–6. The circles are the measured potentials, the solid line is the least-squares fit.

Compared to $Ru_2(ap)_4Cl^{30,35}$ the strongly nucleophilic Ar axial ligand shifts both the $E_{1/2}(Ru_2^{+6/+5})$ and $E_{1/2}(Ru_2^{+5/+4})$ potentials cathodically by an average (of compounds **1–6**) of 350 mV and 300 mV, respectively. Further, the strong e-donor properties of the aryl ligands are reflected in the cathodic shift of the corresponding $E_{1/2}$ values compared to alkynyls. For instance, compared to $Ru_2(ap)_4(C_2Ph)^3$, the $E_{1/2}(Ru_2^{+6/+5})$ of $Ru_2(ap)_4(Ph)$ (**4**) is cathodically shifted by 87 mV, and $E_{1/2}(Ru_2^{+5/+4})$ by 130 mV (see Table S2). As expected, this cathodic shift increases as the *para*-substituent on the aryl ligand becomes increasingly more electrondonating.

Density Functional Theory (DFT) Calculations. In order to gain further insight into the electronic structure of these compounds, the molecular orbitals of compounds 1 and 6, two compounds at the opposite ends of the donicity of *para*-substituents, were computed using spin-restricted DFT. The optimized geometries of 1 and 6 were based on their respective crystal structures. Calculations were performed using the B3LYP functional, and frequency analyses were done to ensure stationary points; resultant structures, namely 1' and 6', are shown in Figure S8, along with optimized metric parameters in Table S9. The bond lengths of the optimized structures are in good agreement with the respective crystal structures. The optimized Ru–Ru bond lengths (ca. 2.39 Å) are ca. 0.06 Å longer than the experimental bond lengths (ca. 2.33 Å). This is attributed to the underestimation of Ru–Ru interactions by the B3LYP functional. On the other hand, the optimized Ru–C bond lengths (ca. 2.17 Å for 1' and 2.19 Å for 6') are shorter than the experimental values (ca. 2.21 Å for 1 and 2.22 for 6). The optimized bond angles were also found to be in good agreement with experiment (Table S9).

The $[Ru_2(ap)_4]^+$ -based compounds generally have three unpaired electrons, and this was indeed confirmed experimentally in compounds 1-6 by room temperature magnetism studies (Evans method, see Experimental Section). This result is also reflected in our computational analyses, which suggests the electronic configuration $\sigma^2 \pi^4 \delta^2 \pi^{*2} \delta^{*1}$. Figure 10 clearly shows that the three singly occupied MOs of 1' and 6' (SOMO, SOMO-1, and SOMO-2) have δ^* , π^* and π^* and character, respectively. The introduction of the aryl ring, as previously described, causes the $\pi^*(Ru_2)$ orbitals to lose their degeneracy, giving rise to the double humped feature seen in the electronic absorption spectra. Whereas SOMO-1 has contributions from both the diruthenium core and the aryl ligand, SOMO-2 has no contribution from the latter, owing to the coplanarity of the d_{vz} orbitals and aryl ligand. DFT calculations support this argument; there is a small but significant difference between the energies of SOMO-1 and SOMO-2 (80 meV for 1 and 30 meV for 6), both of which have $\pi^*(Ru_2)$ character. Both SOMO and LUMO are completely localized on [Ru₂(ap)₄], hence the constant SOMO-LUMO energy gap of 1.74 eV. The crucial difference between 1 and 6 is reflected in their respective SOMO-3 orbitals. As mentioned previously, due to the presence of an electron-donating nitrogen in the para position of the aryl ring in 1 (and 2), SOMO-3 is of $\pi(Ru_2)/\pi(Ar)$ character. On the contrary, SOMO-3 in the case of 6 is localized on $[Ru_2(ap)_4].$

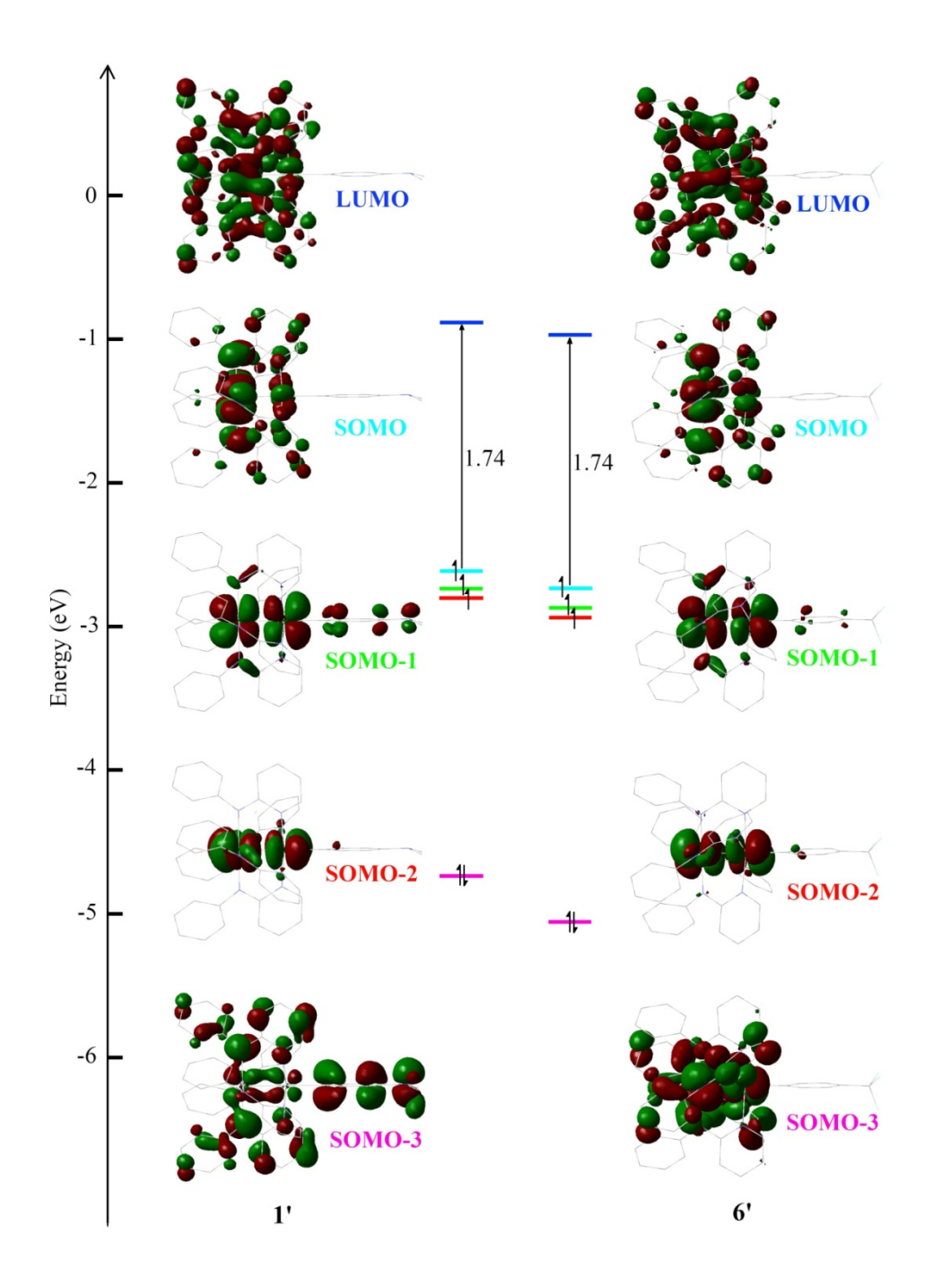


Figure 10. Molecular orbital diagrams for 1' and 6' from DFT calculations.

CONCLUSION

Reported here are the first examples of diruthenium paddlewheel complexes with σ -aryl ligands in the axial sites. The paddlewheel compounds are in the Ru₂⁵⁺ oxidation state, and support up to four electrochemically reversible oxidations, and one reversible reduction, thereby attesting to the remarkable redox stability of such species. Such a quality is highly desired for compounds as the active species in molecular wires / devices. ^{37,38} Additionally, electrochemical studies show that it is possible to tune the reduction potentials of the complexes by altering the substituent on the axial ligand. Overall, the significant cathodic shift in reduction potentials in comparison to their σ -alkynyl counterparts establishes the stronger electron-donor character of the aryl ligand. Further studies of these fundamentally exciting molecules are ongoing.

EXPERIMENTAL SECTION

 $Ru_2(ap)_4Cl^{28,30}$ General. and TPA(OMe)₂Br (4-bromo-N, N-bis(4methoxyphenyl)aniline)³⁹ were prepared using literature methods. ⁿBuLi (2.5 M in hexanes) was purchased from Sigma-Aldrich. All other halogenated ligands were purchased from commercial sources. Tetrahvdrofuran was freshlv distilled over sodium/benzophenone, while dichloromethane was freshly distilled over CaH₂ prior to use. All reactions were performed under dry N₂ atmosphere implementing standard Schlenk procedures unless otherwise noted. UV-Vis/NIR spectra were obtained with a JASCO V-670 spectrophotometer in THF solutions. ¹H NMR spectra were recorded on a Varian Inova 300 spectrometer operating at 300 MHz. Effective magnetic moments (at 25°C) were calculated by Evans method, 40 using ferrocene as the standard. Cyclic and differential pulse voltammograms were recorded in 0.1 M ["Bu₄N][PF₆] solution (CH₂Cl₂, N₂-degassed) on a CHI620A voltammetric analyzer with a glassy carbon working electrode (diameter = 2 mm), a Pt-wire auxiliary electrode, and a Ag/AgCl quasi-reference electrode. The concentration of Ru₂-species is always ca. 1.0 mM. The Fc^{+1/0} couple was observed at ca. 0.417 ± 0.017 V (vs Ag/AgCl) at the noted experimental conditions. Elemental analyses were performed by Atlantic Microlab, Inc.

Synthesis of $Ru_2(ap)_4(C_6H_4-4-NMe_2)$ (1). 4-Bromo-N,N-dimethylanilne (220 mg, 1.1 mmol) was dissolved in 10 mL THF and treated with 0.44 mL of 2.5 M ⁿBuLi (1.1 mmol) at 0°C for 15 min. The aryllithium solution was cannula transferred to a 15 mL THF solution of Ru₂(ap)₄Cl (100 mg, 0.11 mmol). Immediate color change from dark green to black was observed. The reaction mixture was stirred at room temperature for 2h. After removal of solvents, the residue was re-dissolved in a mixture of benzene and ethyl acetate, and the resulting solution as filtered through a deactivated (w/ triethylamine) silica gel pad. The filtrate was collected, solvents were removed, and product was recrystallized from a 1:20 (v:v) CH₂Cl₂:hexanes mixture at -20°C, as a black microcrystalline solid. Yield: 90 mg, 82%. Crystals suitable for X-ray diffraction analysis were grown by layering hexanes over a concentrated solution of 1 in benzene/toluene = 1/1 (v/v). Data for 1. Anal. Found (Calcd.) for $C_{52}H_{48}N_9ORu_2$ (1·H₂O): C, 61.02 (61.40); H, 4.63 (4.76); N, 12.07 (12.39). ESI-MS (m/z, based on 101 Ru): [M⁺] = 999.7. UV-Vis (in THF) λ , nm, (ϵ , M⁻¹cm⁻¹): 464 (5900), 579 (5500), 754 (3500), 831 (3600). R_f (1/5 THF/hexanes (v/v); silica gel deactivated with NEt₃) = 0.32. μ_{eff} (25°C) (Evans method) = 3.9 BM. Electrochemistry (CH₂Cl₂, vs. Fc^{+/0}), $E_{1/2}/V$, $\Delta E_p/mV$, $i_{forward}/i_{backward}$: -0.38, 56, 1.09; 0.12, 57, 1.018; 0.59, 60, ; 0.73, 56, ; -1.62, 63, 1.2.

Synthesis of $Ru_2(ap)_4(C_6H_4-4-N,N-(C_6H_4-4-OMe)_2)$ (2). 4-Bromo-N,N-bis(4-methoxyphenyl)aniline (1.35 g, 3.5 mmol) was dissolved in 15 mL THF and treated with 1.4 mL

of 2.5 M ⁿBuLi (3.5 mmol) at -78°C for 15 min. The temperature was subsequently raised to 0°C, and at this point, a 100 mL THF solution of Ru₂(ap)₄Cl (400 mg, 0.44 mmol) was cannula transferred over to the aryllithium solution. Immediate color change to deep blue-green was observed. The reaction mixture was stirred at room temperature for 2h. After removal of solvent, a blue-green solid was recrystallized from a 1:15 (v:v) THF:hexanes mixture at -20°C. The precipitate was collected on a frit, and rinsed first with hexanes, then cold methanol until the filtrate ran clear. The green residual solid was dried under vacuum. Yield: 491 mg, 95%. Crystals suitable for X-ray diffraction analysis were grown by layering hexanes over a concentrated solution of **2** in EtOAc/benzene = 1/1 (v/v). Data for **2**. Anal. Found (Calcd.) for C₆₄H₅₆N₉O₃Ru₂ (**2**·H₂O): C, 63.97 (63.97); H, 4.75 (4.69); N, 10.26 (10.49). ESI-MS (m/z, based on ¹⁰¹Ru): [M⁺] = 1183.4. UV-Vis (in THF) λ , nm, (ε , M⁻¹cm⁻¹): 464 (6500), 607 (6400), 753 (4200), 822 (4100). R_f (1/5 THF/hexanes (v/v); silica gel deactivated with NEt₃) = 0.2. μ _{eff} (25°C) (Evans method) = 3.8 BM. Electrochemistry (CH₂Cl₂, vs. Fc^{+/0}), E_{1/2}/V, Δ E_p/mV, i_{forward}/i_{backward}: -0.34, 55, 1.18; 0.15, 59, 1.08; 0.59, 59; 0.71, 62, ; -1.58, 1.13.

Synthesis of Ru₂(*ap*)₄(C₆H₄-4-^tBu) (3). 1-Bromo-4-(tert-butyl)benzene (0.218 mL, 1.3 mmol) was dissolved in ca. 15 mL THF and treated with 0.5 mL of 2.5 M ⁿBuLi (1.3 mmol) at 0°C for 15 min. At this point, a 30 mL THF solution of Ru₂(*ap*)₄Cl (115 mg, 0.13 mmol) was cannula transferred over to the aryllithium solution. Immediate color change from dark green to brown-green was observed. The reaction mixture was stirred at room temperature for 2h, during which the solution had acquired a red-brown color. Upon exposure to air, the color of the solution changed back to brown-green. After removal of solvent, a green solid was recrystallized from a 1:15 (v:v) THF:hexanes mixture at -20°C. The precipitate was collected on a frit, and rinsed first with n-pentane, then cold methanol until the filtrate ran clear. The olive-green

residual solid was dried under vacuum. Yield: 85 mg, 67%. Crystals suitable for X-ray diffraction analysis were grown by layering methanol over a concentrated solution of **3** in THF. Data for **3**. Anal. Found (Calcd.) for $C_{54}H_{53}N_8O_2Ru_2\cdot(3\cdot 2H_2O)$: C, 61.94 (61.88); H, 4.80 (5.09); N, 10.63 (10.69). ESI-MS (m/z, based on ^{101}Ru): [M⁺] = 1012.2. UV-Vis (in THF) λ , nm, (ϵ , M⁻¹cm⁻¹): 468 (4900), 643 (1300, sh), 815 (2400). R_f (1/5 THF/hexanes (v/v); silica gel deactivated with NEt₃) = 0.5. μ_{eff} (25°C) (Evans method) = 3.4 BM. Electrochemistry (CH₂Cl₂, vs. Fc^{+/0}), $E_{1/2}/V$, $\Delta E_p/mV$, $i_{forward}/i_{backward}$: -0.31, 57, 1.08; 0.57, irrev.; -1.58, 62, 0.960;

Synthesis of Ru₂(ap)₄(Ph) (4). Bromobenzene (0.092 mL, 0.87 mmol) was dissolved in ca. 10 mL THF and treated with 0.35 mL of 2.5 M ⁿBuLi (0.87 mmol) at 0°C for 15 min. The aryllithium solution was cannula transferred to a 20 mL THF solution of Ru₂(ap)₄Cl (100 mg, 0.11 mmol). Immediate color change from dark green to red-brown was observed. The reaction mixture was stirred at room temperature for 2 h. Upon exposure to air, the color of the solution changed from red-brown to green-brown. After removal of solvent, the crude product mixture was subjected to purification by column chromatography on deactivated (w/ triethylamine) silica. The light green band was eluted (w/ EtOAc/hexanes), and an olive-green microcrystalline solid was isolated. Yield: 32 mg, 30%. Crystals suitable for X-ray diffraction analysis were grown by layering methanol over a concentrated solution of 4 in THF/benzene = 2/1 (v/v). Data for 4. Anal. Found (Calcd.) for C₅₄H₅₁N₈O₃Ru₂ (4·H₂O·EtOAc): C, 61.69 (60.06); H, 4.89 (4.84); N, 10.51 (10.55). ESI-MS (m/z, based on 101 Ru): [M⁺] = 956.1. UV-Vis (in THF) λ , nm (ϵ , M⁻¹cm⁻¹ ¹): 471 (6100), 647 (1700, sh), 812 (3200). R_f (1/5 THF/hexanes (v/v); silica gel deactivated with $NEt_{3}) = 0.39. \ \mu_{eff} \ (25^{\circ}C) \ (Evans \ method) = 4.0 \ BM. \ Electrochemistry \ (CH_{2}Cl_{2}, \ vs. \ Fc^{+/0}), \ E_{1/2}/V, \ (Evans \ method) = 4.0 \ BM. \ Electrochemistry \ (CH_{2}Cl_{2}, \ vs. \ Fc^{+/0}), \ E_{1/2}/V, \ (Evans \ method) = 4.0 \ BM. \ Electrochemistry \ (CH_{2}Cl_{2}, \ vs. \ Fc^{+/0}), \ E_{1/2}/V, \ (Evans \ method) = 4.0 \ BM. \ Electrochemistry \ (CH_{2}Cl_{2}, \ vs. \ Fc^{+/0}), \ E_{1/2}/V, \ (Evans \ method) = 4.0 \ BM. \ Electrochemistry \ (CH_{2}Cl_{2}, \ vs. \ Fc^{+/0}), \ E_{1/2}/V, \ (Evans \ method) = 4.0 \ BM. \ Electrochemistry \ (CH_{2}Cl_{2}, \ vs. \ Fc^{+/0}), \ E_{1/2}/V, \ (Evans \ method) = 4.0 \ BM. \ Electrochemistry \ (CH_{2}Cl_{2}, \ vs. \ Fc^{+/0}), \ E_{1/2}/V, \ (Evans \ method) = 4.0 \ BM. \ Electrochemistry \ (CH_{2}Cl_{2}, \ vs. \ Fc^{+/0}), \ E_{1/2}/V, \ (Evans \ method) = 4.0 \ BM. \ Electrochemistry \ (CH_{2}Cl_{2}, \ vs. \ Fc^{+/0}), \ E_{1/2}/V, \ (Evans \ method) = 4.0 \ BM. \ Electrochemistry \ (CH_{2}Cl_{2}, \ vs. \ Fc^{+/0}), \ E_{1/2}/V, \ (Evans \ method) = 4.0 \ BM. \ Electrochemistry \ (CH_{2}Cl_{2}, \ vs. \ Fc^{+/0}), \ E_{1/2}/V, \ (Evans \ method) = 4.0 \ BM. \ Electrochemistry \ (CH_{2}Cl_{2}, \ vs. \ Fc^{+/0}), \ E_{1/2}/V, \ (Evans \ method) = 4.0 \ BM. \ Electrochemistry \ (CH_{2}Cl_{2}, \ vs. \ Fc^{+/0}), \ E_{1/2}/V, \ (Evans \ method) = 4.0 \ BM. \ Electrochemistry \ (Evans \ method) = 4.0 \ BM. \ Electrochemistry \ (Evans \ method) = 4.0 \ BM. \ Electrochemistry \ (Evans \ method) = 4.0 \ BM. \ Electrochemistry \ (Evans \ method) = 4.0 \ BM. \ Electrochemistry \ (Evans \ method) = 4.0 \ BM. \ Electrochemistry \ (Evans \ method) = 4.0 \ BM. \ Electrochemistry \ (Evans \ method) = 4.0 \ BM. \ Electrochemistry \ (Evans \ method) = 4.0 \ BM. \ Electrochemistry \ (Evans \ method) = 4.0 \ BM. \ Electrochemistry \ (Evans \ method) = 4.0 \ BM. \ Electrochemistry \ (Evans \ method) = 4.0 \ BM. \ Electrochemistry \ (Evans \ method) = 4.0 \ BM. \ Electrochemistry \ (Evans \ method) = 4.0 \ BM. \ Electrochemistry \ (Evans \ method)$ $\Delta E_p/mV$, $i_{forward}/i_{backward}$: -0.30, 57, 1.08; 0.52, 117, 1.37; -1.56, 61, 1.09.

Synthesis of $Ru_2(ap)_4(C_6H_4-4-Br)$ (5). 1-Bromo-4-iodobenzene (832 mg, 2.9 mmol) was dissolved in ca. 25 mL of THF was treated with 1.2 mL of 2.5 M ⁿBuLi (1.4 mmol) at -78°C for 15 min. The temperature was subsequently raised to 0°C, and at this point, a 100 mL THF solution of Ru₂(ap)₄Cl (400 mg, 0.44 mmol) was cannula transferred over to the aryllithium solution. Immediate color change to deep blue-green was observed. The reaction mixture was stirred at room temperature for 2 h. After removal of solvent, the residue was re-dissolved (partially) in hexanes and an olive green solid precipitated out at -20°C. The precipitate was collected on a frit, rinsed with hexanes and cold methanol, and dried under vacuum to afford an olive-green product. Yield: 180 mg, 80%. Crystals suitable for X-ray diffraction analysis were grown by layering hexanes over a concentrated solution of 5 in THF/benzene = 2/1 (v/v). Data for 5. Anal. Found (Calcd.) for C₅₅H₅₀BrCl₂N₈O₂Ru₂ (5·2H₂O·MeOH): C, 55.41 (55.53); H, 3.99 (4.39); N, 9.64 (10.16). ESI-MS (m/z, based on 101 Ru): $[M^{+}] = 1034.9$. UV-Vis (in THF) λ , nm, (ϵ , M⁻¹cm⁻¹): 467 (5700), 650 (1900, sh), 805 (3200). R_f(1/5 THF/hexanes (v/v); silica gel deactivated with NEt₃) = 0.39. μ_{eff} (25°C) (Evans method) = 3.7 BM. Electrochemistry (CH₂Cl₂, vs. $Fc^{+/0}$), $E_{1/2}/V$, $\Delta E_p/mV$, $i_{forward}/i_{backward}$: -0.29, 68, 1.04; 0.53, 63, 1.27; -1.50, 64, 1.06.

Synthesis of Ru₂(*ap*)₄(C₆H₄-4-CF₃) (6). 4-Bromobenzotrifluoride (0.11 mL, 0.77 mmol) was taken in a Schlenk flask and degassed thrice *via* cycles of freeze/pump/thaw, dissolved in ca. 10 mL THF and treated with 0.3 mL of 2.5 M ⁿBuLi at -78°C for 15 min. The aryllithium solution was cannula transferred to a 15 mL THF solution of Ru₂(*ap*)₄Cl (100 mg, 0.11 mmol). Immediate color change from dark green to red-brown was observed. The reaction mixture was stirred at room temperature for 4 h. After 4 h, the color of the solution turned green-brown. After removal of solvent, the crude product mixture was subjected to purification by column chromatography on deactivated (w/ triethylamine) silica. The green band was eluted, and an

olive-green solid was isolated. Yield: 52 mg, 46%. Crystals suitable for X-ray diffraction analysis were grown by layering methanol over a concentrated solution of **6** in THF/benzene = 2/1 (v/v). Data for **6**. Anal. Found (Calcd.) for $C_{55}H_{48}F_3N_8ORu_2$ (**6**·THF): C, 60.76 (60.26); H, 4.68 (4.41); N, 10.47 (10.22). ESI-MS (m/z, based on ^{101}Ru): [M⁺] = 1024.8. UV-Vis (in THF) λ , nm, (ϵ , M⁻¹cm⁻¹): 470 (5600), 661 (2000, sh), 805 (3400). R_f (1/5 THF/hexanes (v/v); silica gel deactivated with NEt₃) = 0.43. μ_{eff} (25°C) (Evans method) = 4.1 BM. Electrochemistry (CH₂Cl₂, vs. Fc^{+/0}), $E_{1/2}/V$, $\Delta E_p/mV$, $i_{forward}/i_{backward}$: -0.24, 62, 1.12; 0.59, 68, 0.90; 0.87, 93, 1.84; -1.47, 64, 1.02.

X-ray Crystallographic Analysis. Single crystal X-ray diffraction data for compounds **1–6** at 100 K were collected on a Bruker AXS D8 Quest CMOS diffractometer using Mo-K α radiation (λ = 0.71073 Å). Data was collected and processed using APEX3,⁴¹ and the structures were solved using SHELXTL^{42,43} suite of programs and refined using Shelxl2016.^{44,45}

Computational Methods. Geometry optimizations of structures 1 and 6 based on the respective crystal structures were done using restricted open-shell density functional theory (DFT)⁴⁶ in dichloromethane. The basis set DGDZVP^{47,48} was used for ruthenium, and 6-31G*⁴⁹⁻⁵³ was used for all other atoms. Frequency analyses were carried out for both the optimized structures 1' and 6', and stationary points were confirmed. All calculations were carried out with the Gaussian 16 suite.⁵⁴

SUPPORTING INFORMATION

The Supporting Information if available free of charge online, and contains the following: Mass

Spectra, Evans method magnetism data, electrochemical data (vs. Ag/AgCl), crystallographic

details (PDF), DFT-optimized structures

CCDC 1879472-1879477 contain the supplementary crystallographic data for this paper. These

data can be obtained free of charge via www.ccdc.cam.ac.uk/data request/cif, by emailing

data request@ccdc.cam.ac.uk, or by contacting The Cambridge Crystallographic Data Centre,

12 Union Road, Cambridge CB2 1EZ, UK; fax: +44 1223 336033.

AUTHOR INFORMATION

Corresponding Author

*E-mail: <u>tren@purdue.edu</u>

ORCID

Tong Ren: 0000-0002-1148-0746

Adharsh Raghavan: 0000-0002-4550-6262

Notes

The authors declare no competing financial interest.

ACKNOWLEDGEMENTS

We thank the National Science Foundation for generously supporting this work (CHE 1764347

for research and CHE 1625543 for X-ray diffractometers).

24

REFERENCES

- (1) Stephenson, T. A.; Wilkinson, G. New Ruthenium carboxylate Complexes. *J. Inorg. Nucl. Chem.* **1966**, *28*, 2285-2291.
- (2) Angaridis, P. In *Multiple Bonds between Metal Atoms*; Third ed.; Cotton, F. A., Murillo, C. A., Walton, R. A., Eds.; Springer Science and Business Media, Inc.: New York, 2005.
- (3) Chakravarty, A. R.; Cotton, F. A. A New Diruthenium(II, III) Compound, Ru₂(CCPh)(PhNpy)₄.2CH₂Cl₂, with an Axial Acetylide Ligand. *Inorg. Chim. Acta* **1986**, *113*, 19-26.
- (4) Ren, T. Diruthenium σ-Alkynyl Compounds: A New Class of Conjugated Organometallics. *Organometallics* **2005**, *24*, 4854-4870.
- (5) Bear, J. L.; Han, B.; Huang, S. Molecular Structure and Electrochemistry of Ru2(dpf)4(CCPh)2: A Novel Ru(III)-Ru(III) Dimer. *J. Am. Chem. Soc.* **1993**, *115*, 1175-1177.
- (6) Bear, J. L.; Han, B.; Huang, S.; Kadish, K. M. Effect of Axial Ligands on the Oxidation State, Structure, and Electronic Configuration of Diruthenium Complexes. *Inorg. Chem.* **1996**, *35*, 3012-3021.
- (7) Ren, T.; Zou, G.; Alvarez, J. C. Facile electronic communication between bimetallic termini bridged by elemental carbon chains. *Chem. Commun.* **2000**, 1197-1198.
- (8) Wong, K.-T.; Lehn, J.-M.; Peng, S.-M.; Lee, G.-H. Nanoscale molecular organometallo-wires containing diruthenium cores. *Chem. Commun.* **2000**, 2259-2260.
- (9) Blum, A. S.; Ren, T.; Parish, D. A.; Trammell, S. A.; Moore, M. H.; Kushmerick, J. G.; Xu, G.-L.; Deschamps, J. R.; Pollack, S. K.; Shashidhar, R. Ru₂(ap)₄(σ-oligo(phenyleneethynyl)) Molecular Wires: Synthesis and Electronic Characterization. *J. Am. Chem. Soc.* **2005**, *127*, 10010-10011.
- (10) Kuo, C.; Chang, J.; Yeh, C.; Lee, G.; Wang, C.; Peng, S. Synthesis, structures, magnetism and electrochemical properties of triruthenium-acetylide complexes. *Dalton Trans.* **2005**, 3696-3701.
- (11) Mahapatro, A. K.; Ying, J.; Ren, T.; Janes, D. B. Electronic Transport through Ruthenium Based Redox-Active Molecules in Metal-Molecule-Metal Nanogap Junctions. *Nano Lett* **2008**, *8*, 2131-2136.
- (12) Zhu, H.; Pookpanratana, S. J.; Bonevich, J. E.; Natoli, S. N.; Hacker, C. A.; Ren, T.; Suehle, J. S.; Richter, C. A.; Li, Q. Redox-Active Molecular Nanowire Flash Memory for High-Endurance and High-Density Nonvolatile Memory Applications. *ACS Appl. Mater. Inter.* **2015**, *7*, 27306-27313.
- (13) Pookpanratana, S.; Zhu, H.; Bittle, E. G.; Natoli, S. N.; Ren, T.; Richter, C. A.; Li, Q.; Hacker, C. A. Non-volatile memory devices with redox-active diruthenium molecular compound. *J. Phys.-Condens. Mat.* **2016**, *28*.
- (14) Corcos, A. R.; Pap, J. S.; Yang, T.; Berry, J. F. A Synthetic Oxygen Atom Transfer Photocycle from a Diruthenium Oxyanion Complex. *J. Am. Chem. Soc.* **2016**, *138*, 10032-10040.
- (15) Corcos, A. R.; Roy, M. D.; Killian, M. M.; Dillon, S.; Brunold, T. C.; Berry, J. F. Electronic Structure of Anilinopyridinate-Supported Ru25+ Paddlewheel Compounds. *Inorg. Chem.* **2017**, *56*, 14662-14670.
- (16) Corcos, A. R.; Berry, J. F. Capturing the missing AgF2 (-) anion within an Ru-2(III/III) dimeric dumbbell complex. *Dalton Trans.* **2016**, *45*, 2386-2389.
- (17) Bear, J. L.; Chen, W. Z.; Han, B. C.; Huang, S. R.; Wang, L. L.; Thuriere, A.; Van Caemelbecke, E.; Kadish, K. M.; Ren, T. Cyanide adducts on the diruthenium core of Ru-2(L)(4) (+) (L = ap, CH(3)ap, Fap, or F(3)ap). Electronic properties and binding modes of the bridging ligand. *Inorg. Chem.* **2003**, *42*, 6230-6240.
- (18) Manowong, M.; Han, B.; McAloon, T. R.; Shao, J.; Guzei, I. A.; Ngubane, S.; Caemelbecke, E. V.; Bear, J. L.; Kadish, K. M. Effect of Axial Ligands on the Spectroscopic and Electrochemical Properties of Diruthenium Compounds. *Inorg. Chem.* **2014**, *53*, 7416-7428.
- (19) Nichols, J. M.; Wolf, J.; Zavalij, P.; Varughese, B.; Doyle, M. P. Bis(phenyl)dirhodium(III) Caprolactamate: A Dinuclear Paddlewheel Complex with No Metal-Metal Bond. *J. Am. Chem. Soc.* **2007**, *129*, 3504-3505.
- (20) Xie, J.-H.; Zhou, L.; Lubek, C.; Doyle, M. P. Hetero-bis(ó-aryl)dirhodium(III) caprolactamates. Electronic communication between aryl groups through dirhodium(III). *Dalton Trans.* **2009**, 2871.

- (21) Angelone, D.; Draksharapu, A.; Browne, W. R.; Choudhuri, M. M. R.; Crutchley, R. J.; Xu, X.; Xu, X.; Doyle, M. P. Dinuclear compounds without a metal-metal bond. Dirhodium(III,III) carboxamidates. *Inorg. Chim. Acta* **2015**, *424*, 235-240.
- Wolf, J.; Poli, R.; Xie, J.-H.; Nichols, J.; Xi, B.; Zavalij, P.; Doyle, M. P. Removal of Metal-Metal Bonding in a Dimetallic Paddlewheel Complex: Molecular and Electronic Structure of Bis(phenyl) Dirhodium(III) Carboxamidate Compounds. *Organometallics* **2008**, *27*, 5836-5845.
- (23) Bear, J. L.; Han, B.; Li, Y.; Ngubane, S.; Van Caemelbecke, E.; Kadish, K. M. Synthesis, spectroscopic properties and electrochemistry of $Rh_2(ap)_4(R)$ where $R=CH_3$ or C_6H_5 and ap=2-anilinopyridinate anion. *Polyhedron* **2009**, *28*, 1551-1555.
- (24) Cabeza, J. A.; del Rio, I.; Garcia-Granda, S.; Riera, V.; Suarez, M. Reactivity of a triruthenium cluster complex containing a mu(3)-eta(3)(C,N-2) ligand derived from 2-amino-7,8-benzoquinoline. Coupling of this ligand with C-3 fragments and characterization of mu(3)-vinylidene and mu-stannylene derivatives. *Organometallics* **2004**, *23*, 3501-3511.
- (25) Briard, P.; Cabeza, J. A.; Llamazares, A.; Ouhab, L.; Riera, V. Synthesis and Structural Characterization of Triruthenium Cluster Complexes Containing Bridging Eta(1)-Phenyl and Terminal Eta(1)-Phenyl Ligands Arising from the Cleavage of Triphenylphosphine Ligands. *Organometallics* **1993**, *12*, 1006-1008.
- (26) Chakravarty, A. R.; Cotton, F. A.; Tocher, D. A. Displacive Transfer of a Phenyl Group from Triphenylphosphine to a Metal Atom: Synthesis and Molecular Structure of Ru₂Ph₂(PhCONH)₂[Ph₂POC(Ph)N]₂. J. Am. Chem. Soc. **1984**, 106, 6409-6413.
- (27) Chakravarty, A. R.; Cotton, F. A. The Aryl Group Transfer Process From a Triarylphosphine to a Chlorotetrakis(Amidato)Diruthenium(II,III) Species Syntheses and Molecular-Structures of $Ru_2(R)_2(R'Conh)_2[R_2poc(R')N]_2$ ($R = C_6H_5$, $R'=3,5-(OCH_3)_2C_6H_3-R=para-C_6H_4CH_3$, $R'=C_6H_5$). *Inorg. Chem.* **1985**, *24*, 3584-3589.
- (28) Chakravarty, A. R.; Cotton, F. A.; Tocher, D. A. Syntheses, Molecular Structures, and Properties of Two Polar Diruthenium(II,III) Complexes of 2-Hydroxypyridine and 2-Anilinopyridine. *Inorg. Chem.* **1985**, *24*, 172-177.
- (29) Cordero, B.; Gómez, V.; Platero-Prats, A. E.; Revés, M.; Echeverría, J.; Cremades, E.; Barragán, F.; Alvarez, S. Covalent radii revisited. *J. Chem. Soc., Dalton Trans.* **2008**, 2832-2838.
- (30) Zou, G.; Alvarez, J. C.; Ren, T. Ru-σ-Alkynyl Compounds of Tetraanilinopyridinato-diruthenium(II,III) Core: Synthesis and Structural Characterization. *J. Organomet. Chem.* **2000**, *596*, 152-158.
- (31) Hansch, C.; Leo, A.; Taft, R. W. A survey of Hammett substituent constants and resonance and field parameters. *Chem. Rev.* **1991**, *91*, 165-195.
- (32) Dapperheld, S.; Steckhan, E.; Brinkhaus, K. H. G.; Esch, T. Organic Electron Transfer Systems, II. Substituted Triarylamine Cation-Radical Redox Systems Synthesis, Electrochemical and Spectroscopic Properties, Hammet Behavior, and Suitability as Redox Catalysts. *Chem. Ber.* **1991**, *124*, 2557-2567.
- (33) Ren, T. Substituent effects in dinuclear paddlewheel compounds: electrochemical and spectroscopic investigations. *Coordination Chemistry Reviews* **1998**, *175*, 43-58.
- (34) Hurst, S. K.; Xu, G. L.; Ren, T. Bis-adducts of substituted phenylethynyl on a Ru₂(DMBA)₄ core: Effect of donor/acceptor modifications. *Organometallics* **2003**, *22*, 4118-4123.
- (35) Chakravarty, A. R.; Cotton, F. A.; Tocher, D. A.; Tocher, J. H. Electrochemical Studies on Three Polar Diruthenium(II,III) Complexes. *Polyhedron* **1985**, *4*, 1475-1478.
- (36) Cummings, S. P.; Cao, Z.; Fanwick, P. E.; Kharlamova, A.; Ren, T. Diruthenium(III,III) ethynylphenyleneimine molecular wires: Preparation via on-complex Schiff base condensation. *Inorg. Chem.* **2012**, *51*, 7561-7568.
- (37) Xiang, D.; Wang, X.; Jia, C.; Lee, T.; Guo, X. Molecular-Scale Electronics: From Concept to Function. *Chem. Rev.* **2016**, *116*, 4318-4440.
- (38) Zhang, X.-Y.; Zheng, Q. Q.; Chen-Xi, Q.; Zuo, J.-L. Some New Progress on Molecular Wires. *Chinese J. Inorg. Chem.* **2011**, *27*, 1451-1464.

- (39) Mengel, A. K. C.; He, B.; Wenger, O. S. A triarylamine-triarylborane dyad with a photochromic dithienylethene bridge. *J. Org. Chem.* **2012**, *77*, 6545-6552.
- (40) Evans, D. F. The Determination of the Pararnagnetic Susceptibility of Substances in Solution by Nuclear Magnetic Resonance. *J. Chem. Soc.* **1959**, *0*, 2003-2005.
- (41) Bruker, Apex3 v2016.9-0, Saint V8.34A, Saint V8.37A; Bruker AXS Inc.: Madison, WI, 2016.
- (42) SHELXTL, version 6.14; Bruker Advanced X-ray Solutions, Bruker AXS Inc.: Madison, WI, 2000-2003.
- (43) Sheldrick, G. M. A short history of SHELX. Acta Cryst. 2008, 64, 112-122.
- (44) Sheldrick, G. M. SHELXL 2016; University of Göttingen, Germany, 2016. 2016.
- (45) Sheldrick, G. M. Crystal structure refinement with SHELXL. *Acta Cryst. C* **2015**, 71, 3-8.
- (46) Parr, R. G. Y., W. *Density Functional Theory of Atoms and Molecules*; Oxford University Press: New York, 1989.
- (47) N. Godbout; D. R. Salahub; J. Andzelm; Wimmer, E. Optimization of Gaussian-type basis sets for local spin density functional calculations. Part I. Boron through neon, optimization technique and validation. *Can. J. Chem.* **1992**, *70*, 560-71.
- (48) C. Sosa, J. A., B. C. Elkin, E. Wimmer, K. D. Dobbs, and D. A. Dixon A Local Density Functional Study of the Structure and Vibrational Frequencies of Molecular Transition-Metal Compounds. *J. Phys. Chem.* **1992**, *96*, 6630-36.
- (49) M. M. Francl, W. J. P., W. J. Hehre, J. S. Binkley, D. J. DeFrees, J. A. Pople, and M. S. Gordon Self-Consistent Molecular Orbital Methods. 23. A polarization-type basis set for 2nd-row elements. *J. Chem. Phys.* **1982**, *77*, 3654-65.
- (50) R. Ditchfield, W. J. H., and J. A. Pople Self-Consistent Molecular Orbital Methods. 9. Extended Gaussian-type basis for molecular-orbital studies of organic molecules. *J. Chem. Phys.* **1971**, *54*, 724.
- (51) W. J. Hehre, R. D., J. A. Pople Self-Consistent Molecular Orbital Methods. 12. Further extensions of Gaussian-type basis sets for use in molecular-orbital studies of organic-molecules. *J. Chem. Phys.* **1972**, *56*, 2257.
- (52) P. C. Hariharan; Pople, J. A. Influence of polarization functions on molecular-orbital hydrogenation energies. *Theor. Chem. Acc.* **1973**, *28*, 213-22.
- (53) Hariharan, P. C.; Pople, J. A. Accuracy of AH equilibrium geometries by single determinant molecular-orbital theory. *Mol. Phys.* **1974**, *27*, 209-14.
- (54) *Gaussian 16 Rev. B.01*; Frisch, M. J.; Trucks, G. W.; Schlegel, H. B.; Scuseria, G. E.; Robb, M. A.; Cheeseman, J. R.; Scalmani, G.; Barone, V.; Petersson, G. A.; Nakatsuji, H.; Li, X.; Caricato, M.; Marenich, A. V.; Bloino, J.; Janesko, B. G.; Gomperts, R.; Mennucci, B.; Hratchian, H. P.; Ortiz, J. V.; Izmaylov, A. F.; Sonnenberg, J. L.; Williams; Ding, F.; Lipparini, F.; Egidi, F.; Goings, J.; Peng, B.; Petrone, A.; Henderson, T.; Ranasinghe, D.; Zakrzewski, V. G.; Gao, J.; Rega, N.; Zheng, G.; Liang, W.; Hada, M.; Ehara, M.; Toyota, K.; Fukuda, R.; Hasegawa, J.; Ishida, M.; Nakajima, T.; Honda, Y.; Kitao, O.; Nakai, H.; Vreven, T.; Throssell, K.; Montgomery Jr., J. A.; Peralta, J. E.; Ogliaro, F.; Bearpark, M. J.; Heyd, J. J.; Brothers, E. N.; Kudin, K. N.; Staroverov, V. N.; Keith, T. A.; Kobayashi, R.; Normand, J.; Raghavachari, K.; Rendell, A. P.; Burant, J. C.; Iyengar, S. S.; Tomasi, J.; Cossi, M.; Millam, J. M.; Klene, M.; Adamo, C.; Cammi, R.; Ochterski, J. W.; Martin, R. L.; Morokuma, K.; Farkas, O.; Foresman, J. B.; Fox, D. J.: Wallingford, CT, 2016.

SYNOPSIS

The first examples of Ru– C_{sp^2} bonds in paddlewheel complexes are reported. Employing the lithium-halogen exchange reaction, six new compounds of the form Ru₂(ap)₄(Ar) (ap=2-anlinipyridinate; Ar = aryl) have been synthesized, and characterized via mass spectrometry, electronic absorption spectroscopy, electrochemistry and magnetism studies. Their molecular structures have been confirmed using single crystal X-ray diffraction analysis.

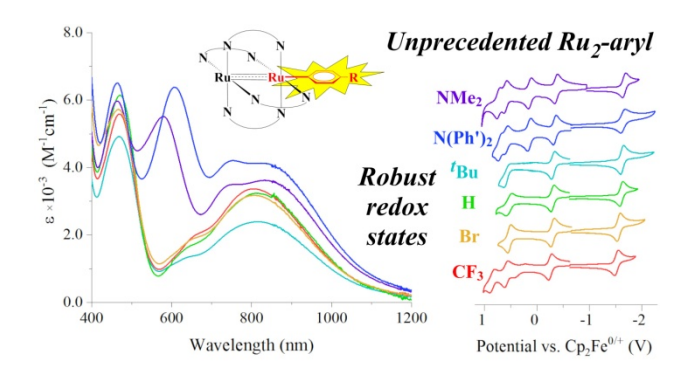


Figure TOC. For Table of Contents only.